

# Protein Carbonylation of an Amino Acid Residue of the Na/K-ATPase $\alpha$ 1 Subunit Determines Na/K-ATPase Signaling and Sodium Transport in Renal Proximal Tubular Cells

Yanling Yan, PhD; Anna P. Shapiro, MD; Brahma R. Mopidevi, PhD; Muhammad A. Chaudhry, PhD; Kyle Maxwell, BSci; Steven T. Haller, PhD; Christopher A. Drummond, PhD; David J. Kennedy, PhD; Jiang Tian, PhD; Deepak Malhotra, MD, PhD; Zi-jian Xie, PhD; Joseph I. Shapiro, MD; Jiang Liu, MD, PhD

**Background**—We have demonstrated that cardiotonic steroids, such as ouabain, signaling through the Na/K-ATPase, regulate sodium reabsorption in the renal proximal tubule. By direct carbonylation modification of the Pro222 residue in the actuator (A) domain of pig Na/K-ATPase  $\alpha$ 1 subunit, reactive oxygen species are required for ouabain-stimulated Na/K-ATPase/c-Src signaling and subsequent regulation of active transepithelial  $^{22}\text{Na}^+$  transport. In the present study we sought to determine the functional role of Pro222 carbonylation in Na/K-ATPase signaling and sodium handling.

**Methods and Results**—Stable pig  $\alpha$ 1 knockdown LLC-PK1-originated PY-17 cells were rescued by expressing wild-type rat  $\alpha$ 1 and rat  $\alpha$ 1 with a single mutation of Pro224 (corresponding to pig Pro222) to Ala. This mutation does not affect ouabain-induced inhibition of Na/K-ATPase activity, but abolishes the effects of ouabain on Na/K-ATPase/c-Src signaling, protein carbonylation, Na/K-ATPase endocytosis, and active transepithelial  $^{22}\text{Na}^+$  transport.

**Conclusions**—Direct carbonylation modification of Pro224 in the rat  $\alpha$ 1 subunit determines ouabain-mediated Na/K-ATPase signal transduction and subsequent regulation of renal proximal tubule sodium transport. (*J Am Heart Assoc.* 2016;5:e003675 doi: 10.1161/JAHA.116.003675)

**Key Words:** Na/K-ATPase • protein carbonylation • protein trafficking • reactive oxygen species • signaling • sodium transport

**B**inding of ouabain, one of the cardiotonic steroids, to the Na/K-ATPase  $\alpha$ 1 subunit stimulates multiple protein kinase signaling cascades. One of the downstream effects of ouabain-stimulated Na/K-ATPase signaling is Ras-dependent superoxide-related reactive oxygen species (ROS) generation, which is an integrated component of ouabain-mediated Na/K-ATPase signaling.<sup>1,2</sup> We have reported that cardiotonic steroids stimulate ROS generation in different in vitro and in vivo models and also that increases in  $\text{H}_2\text{O}_2$  activate Na/K-

ATPase signaling pathways and promote Na/K-ATPase endocytosis.<sup>1–8</sup>

The effect of ROS on the Na/K-ATPase activity has been well documented.<sup>9–12</sup> Oxidative modification, such as glutathionylation of cysteine residue(s) of the Na/K-ATPase  $\alpha$ 1 subunit<sup>11</sup> and  $\beta$ 1 subunit,<sup>10</sup> inhibits the Na/K-ATPase activity by either stabilizing the enzyme in an E2-prone conformation or by blocking the ATP-binding site. We have reported that while ouabain stimulates ROS generation via the Ras/Rac cascade of the Na/K-ATPase signaling pathways, increases in ROS also activate the Na/K-ATPase signaling, allowing the formation of a Na/K-ATPase/Src/ROS signaling amplification loop.<sup>1–6,8,13</sup> Recently, we have further demonstrated that ROS causes direct protein carbonylation of Pro222 of the actuator (A) domain of the  $\alpha$ 1 subunit of Na/K-ATPase in pig LLC-PK1 cells.<sup>6</sup> This carbonylation modification process is dependent on c-Src activation as demonstrated by using the Src-deficient SYF and c-Src reconstituted SYF+c-Src cells.<sup>6</sup> Functionally, ouabain and increases in  $\text{H}_2\text{O}_2$  stimulate Na/K-ATPase signaling, protein carbonylation, and redistribution of Na/K-ATPase and NHE3, leading to the inhibition of active transepithelial  $^{22}\text{Na}^+$  flux.<sup>6</sup>

From the Department of Pharmacology, Physiology and Toxicology, JCE School of Medicine (Y.Y., M.A.C., K.M., J.I.S., J.L.) and Marshall Institute for Interdisciplinary Research (Z.-j.X., J.L.), Marshall University, Huntington, WV; Department of Medicine, University of Toledo College of Medicine, Toledo, OH (A.P.S., B.R.M., S.T.H., C.A.D., D.J.K., J.T., D.M., J.I.S.).

**Correspondence to:** Jiang Liu, MD, PhD, Department of Pharmacology, Physiology and Toxicology, Joan C. Edwards School of Medicine at Marshall University, One John Marshall Dr, Huntington, WV 25755.

E-mail: liuj@marshall.edu

Received April 4, 2016; accepted August 12, 2016.

© 2016 The Authors. Published on behalf of the American Heart Association, Inc., by Wiley Blackwell. This is an open access article under the terms of the Creative Commons Attribution-NonCommercial License, which permits use, distribution and reproduction in any medium, provided the original work is properly cited and is not used for commercial purposes.

Our in vitro data suggest that protein carbonylation of Na/K-ATPase  $\alpha$ 1 subunit may be a novel regulatory mechanism of Na/K-ATPase signaling. However, the functional role of Pro222 carbonylation in the Na/K-ATPase signaling is unclear. We report here that mutation of Pro224 (as Pro222 in pig  $\alpha$ 1) to Ala in the rat  $\alpha$ 1 subunit does not affect ouabain-induced inhibition of the Na/K-ATPase activity, but the mutation abolishes ouabain-induced Na/K-ATPase signaling, protein carbonylation, endocytosis of the Na/K-ATPase, and inhibition of active transepithelial  $^{22}\text{Na}^+$  transport. Taken together, we suggest that Pro224 of rat  $\alpha$ 1 dictates the renal proximal tubule (RPT) Na/K-ATPase signaling and sodium transport, and that carbonylation modification of Pro224 functions as a signaling amplifier of Na/K-ATPase signaling.

## Materials and Methods

### Chemicals and Antibodies

All chemicals, except otherwise mentioned, were obtained from Sigma-Aldrich (St. Louis, MO). Monoclonal antibodies against Na/K-ATPase  $\alpha$ 1 subunit (clone  $\alpha$ 6F and clone C464.6) and  $\beta$ 1 (clone C464.8) were from the Developmental Studies Hybridoma Bank at the University of Iowa (Iowa City, IA) and EMD Millipore Upstate (Billerica, MA), respectively. Polyclonal anti-rat  $\alpha$ 1-specific antibody (anti-NASE) was kindly provided by Dr Pressley (Texas Tech University Health Sciences Center, Lubbock, TX). Polyclonal antibody against early endosome marker Rab5 was from Cell Signaling Technology (Danvers, MA). Polyclonal anti-Src (pY418) phosphospecific antibody was from Invitrogen (Camarillo, CA). Monoclonal antibodies against total c-Src and tyrosine phosphorylation (p-Tyr, clone PY99) were from Santa Cruz (Santa Cruz, CA). 2,4-Dinitrophenylhydrazine and antibody against 2,4-dinitrophenyl hydrazone derivatives were from Sigma-Aldrich. Radioactive [ $^3\text{H}$ ]-ouabain,  $^{86}\text{RbCl}$ , and  $^{22}\text{NaCl}$  were from Perkin Elmer (Shelton, CA).

### Cell Cultures

Cells were cultured with Dulbecco's modified Eagle's medium with 10% fetal bovine serum, 100 U/mL penicillin, and 100  $\mu\text{g}/\text{mL}$  streptomycin, in a 5%  $\text{CO}_2$ -humidified incubator. Culture medium was changed daily until confluence. Cells were serum-starved for 16 to 18 hours before treatment. In assays for active transcellular  $^{22}\text{Na}^+$  flux, cells were grown on Transwell<sup>®</sup> membrane support (Costar Transwell<sup>®</sup> culture filter inserts, filter pore size: 0.4  $\mu\text{m}$ ; Costar, Cambridge, MA) to form monolayers. The transcellular epithelial electrical resistance was measured with EVOM2 Epithelial VoltOhmmeter system (World Precision Instruments, Sarasota, FL).

## Generation of Mutant Cells

For the present study, neither a protocol approved by Institutional Review Board nor a protocol approved by institutional Animal Care and Use Committee was required. The wild-type AAC-19 cells as well as mutant P224A and A416P cells were all generated from PY-17 cells by using pRc/CMV1-rat  $\alpha$ 1 plasmid that was also kindly provided by Dr Pressley. The PY-17 is a stable cell line, generated from pig LLC-PK1 cells, with knockdown of pig  $\alpha$ 1 by siRNA method. The PY-17 cells only expressed  $\approx$ 8% to 10% of pig  $\alpha$ 1 compared to parent LLC-PK1 cells.<sup>14,15</sup> The pRc/CMV1-rat  $\alpha$ 1 plasmid has been used to develop several stable cell lines including rat  $\alpha$ 1 rescued AAC-19 (expressing full-length wild-type rat  $\alpha$ 1<sup>14,15</sup>) and A416P cells (expressing Ala416/Pro416 mutation in rat  $\alpha$ 1<sup>16</sup>). The mutant P224A stable cell line (expressing Pro224/Ala224 mutation in rat  $\alpha$ 1) was generated in the same way as generation of A416P cells. The LLC-PK1 cells were used to evaluate the total  $\alpha$ 1 expression level, and the PY-17 cells were used to evaluate the expression level of endogenous pig  $\alpha$ 1 in AAC-19, P224A, and A416P cells.

The Pro222 of pig  $\alpha$ 1 (UniProtKB/Swiss-Prot No P05024) in LLC-PK1 cells corresponds to the Pro224 of the rat  $\alpha$ 1 (No P06685, Table 1). Site-directed mutagenesis was used to convert Pro224 of rat  $\alpha$ 1 to generate single Pro224/Ala224 mutation with the QuikChange II Site-Directed Mutagenesis Kit (Stratagene, Santa Clara, CA). The mutated sequence was confirmed by DNA sequencing. To develop stable cell lines, transfected ouabain-resistant colonies were selected with ouabain (3  $\mu\text{mol}/\text{L}$ ) for 1 week post-transfection to eliminate endogenous ouabain-sensitive pig  $\alpha$ 1 as well as untransfected PY-17 cells because pig  $\alpha$ 1 subunit is highly sensitive to ouabain compared to rat  $\alpha$ 1.<sup>17</sup> Survived colonies expressing rat  $\alpha$ 1 mutants were expanded into single-cell stable cell lines and verified by specific anti-rat  $\alpha$ 1 antibody (anti-NASE) and [ $^3\text{H}$ ] ouabain binding assay. Wild-type rat  $\alpha$ 1-rescued PY-17 cell, AAC-19, was used for control in the following studies.

**Table 1.** Partial Alignment of the  $\alpha$ 1 Subunit

SP P05023  AT1A1_HUMAN	181 CKVDNSSLTGESEP <sup>224</sup> QTRSPDFTNENPLETR 240
SP P05024  AT1A1_PIG	179 CKVDNSSLTGESEP <sup>222</sup> QTRSPDFTNENPLETR 238
SP P06685  AT1A1_RAT	181 CKVDNSSLTGESEP <sup>224</sup> QTRSPDFTNENPLETR 240
SP Q8VDN2  AT1A1_MOUSE	181 CKVDNSSLTGESEP <sup>224</sup> QTRSPDFTNENPLETR 240

The sequences were obtained from UniProtKB/Swiss-Prot.

## Isolation of Early Endosome (EE) Fractions

The EE fractions were isolated by sucrose flotation centrifugation, and the enrichment of EE fractions was verified by the EE marker Rab5 as we previously described.<sup>18,19</sup> An equal amount of total protein from each sample was precipitated with trichloroacetic acid for Western blot analysis of Na/K-ATPase  $\alpha$ 1 and  $\beta$ 1 subunits. After immunoblotting with the  $\alpha$ 1 and  $\beta$ 1 subunits, the same membrane was stripped and immunoblotted for Rab5 to serve as loading control. Endocytosed  $\alpha$ 1 and  $\beta$ 1 subunits were normalized by Rab5.

## [<sup>3</sup>H]-Ouabain Binding Assay

To evaluate the cell surface expression level of endogenous pig Na/K-ATPase  $\alpha$ 1 subunit, [<sup>3</sup>H]-ouabain binding assay was performed as described before.<sup>16</sup> The [<sup>3</sup>H]-ouabain binding was calibrated with protein content and expressed as the percentage of pig  $\alpha$ 1 knockdown PY-17 cells. Each experiment was performed in triplicate.

## Enzymatic and Ion-Exchange Activity Assays

The enzymatic activity of the Na/K-ATPase was performed by using BIOMOL GREEN Reagent (Enzo Life Science) as described in<sup>16</sup>. Briefly, cells were homogenized, briefly sonicated, and centrifuged (800g for 10 minutes) in ice-cold buffer A (150 mmol/L sucrose, 5 mmol/L HEPES, 4 mmol/L EGTA, 0.8 mmol/L dithiothreitol, pH 7.4). The crude membrane pellet was obtained after centrifugation of the postnuclear fraction (45 000g for 45 minutes) and was resuspended in buffer A to determine protein concentration. The crude membrane samples were treated with alamethicin (0.1 mg/mg of protein) for 10 minutes at room temperature and then added to the buffer B (50 mmol/L Tris, 1 mmol/L EGTA, 1 mmol/L MgCl<sub>2</sub>, 25 mmol/L KCl, 100 mmol/L NaCl, 5 mmol/L NaN<sub>3</sub>, pH 7.4). After 15 minutes of pre-incubation at 37°C, the reaction was started by adding ATP/Mg<sup>2+</sup> (final concentration of 2 mmol/L) and continued for 45 minutes, and then stopped by adding 8% ice-cold trichloroacetic acid. Phosphate generated during the ATP hydrolysis was measured by BIOMOL GREEN Reagent. Ouabain-sensitive Na/K-ATPase activities were calculated as the difference between the presence and absence of 1 mmol/L ouabain.

To evaluate the transport activity of the Na/K-ATPase and NHE3, <sup>86</sup>Rb<sup>+</sup> and H<sup>+</sup>-driven <sup>22</sup>Na<sup>+</sup> uptake were performed as previously described.<sup>18,20</sup> Prior to the initiation of the <sup>86</sup>Rb<sup>+</sup> uptake assay, cellular Na<sup>+</sup> was “clamped” with 20  $\mu$ mol/L monensin for 15 minutes to assure the measurement of the maximal capacity of total active <sup>86</sup>Rb<sup>+</sup> uptake and to minimize the potential effect of changes in intracellular Na<sup>+</sup>. The assay was stopped 10 minutes after adding <sup>86</sup>Rb<sup>+</sup> ( $\approx$ 1  $\mu$ Ci/mL

medium) by washing 3 times with ice-cold 100 mmol/L MgCl<sub>2</sub> solution. In parallel, ouabain-insensitive <sup>86</sup>Rb<sup>+</sup> uptake (pretreated with 2 mmol/L ouabain for 15 minutes) was measured in the presence of monensin. Ouabain-sensitive <sup>86</sup>Rb<sup>+</sup> uptake was calculated by subtraction of ouabain-insensitive <sup>86</sup>Rb<sup>+</sup> uptake from total <sup>86</sup>Rb<sup>+</sup> uptake. Prior to H<sup>+</sup>-driven <sup>22</sup>Na<sup>+</sup> uptake assay, cells were pretreated with 50  $\mu$ mol/L amiloride for 30 minutes to inhibit amiloride-sensitive NHE1 activity without significant inhibition of NHE3<sup>20,21</sup> and Na/K-ATPase.<sup>22</sup> This allows the measurement of acid-stimulated Na<sup>+</sup> entry mainly mediated through apical NHE3. To determine H<sup>+</sup>-driven <sup>22</sup>Na<sup>+</sup> uptake, after treated with or without ouabain (10  $\mu$ mol/L, 1 hour), cells were first rinsed 3 times with Na<sup>+</sup>-free buffer (in mmol/L, *N*-methyl-D-glucamine [NMDG<sup>+</sup>] Cl 140, KCl 4, MgCl<sub>2</sub> 2, CaCl<sub>2</sub> 1, and HEPES 10, pH 7.4) and acid loaded for 10 minutes in ammonium-containing Na<sup>+</sup>-free buffer in which 30 mmol/L NMDG<sup>+</sup> was replaced with 30 mmol/L NH<sub>4</sub>Cl (in mmol/L, NMDGCl 110, NH<sub>4</sub>Cl 30, KCl 4, MgCl<sub>2</sub> 2, CaCl<sub>2</sub> 1, and HEPES 10, pH 7.4). The <sup>22</sup>Na<sup>+</sup> uptake was initiated by replacing the NH<sub>4</sub><sup>+</sup>-containing buffer with Na<sup>+</sup>-free buffer containing 2 mmol/L <sup>22</sup>NaCl ( $\approx$ 1  $\mu$ Ci/mL buffer). The <sup>22</sup>Na<sup>+</sup> uptake was stopped after 4 minutes by washing 4 times with ice-cold saline. Each experiment was performed in triplicate.

To determine the effect of ouabain (10  $\mu$ mol/L, 1 hour) on Na/K-ATPase transport capacity, cells were pretreated with or without ouabain (10  $\mu$ mol/L, 1 hour) prior to the assays. Since rat  $\alpha$ 1 subunit is ouabain-resistant compared to pig  $\alpha$ 1 subunit, we chose 10  $\mu$ mol/L of ouabain that is able to stimulate Na/K-ATPase/c-Src signaling in rat RPT primary cultures.<sup>23</sup>

## Active Transepithelial <sup>22</sup>Na<sup>+</sup> Flux Assay

Cells were cultured on Transwell<sup>®</sup> membrane support to form monolayers and pretreated with 50  $\mu$ mol/L amiloride for 30 minutes to inhibit amiloride-sensitive NHE1 activity. Active transepithelial <sup>22</sup>Na<sup>+</sup> flux (from apical to basolateral compartment) was determined by counting radioactivity in the basolateral aspect 1 hour after <sup>22</sup>Na<sup>+</sup> addition to the apical compartment as previously described.<sup>18</sup> Each experiment was performed in triplicate.

To determine the effect of ouabain (10  $\mu$ mol/L, 1 hour) on transepithelial <sup>22</sup>Na<sup>+</sup> transport capacity, cells were pretreated with or without ouabain (10  $\mu$ mol/L, 1 hour) in basolateral compartments prior to the <sup>22</sup>Na<sup>+</sup> flux assay.

## Assessment of Phosphorylation of Tyrosine, c-Src, and ERK1/2

Cells were treated with and without ouabain (10  $\mu$ mol/L, 1 hour). Whole cell lysates were prepared with Nonidet P-40

buffer (containing 1% Nonidet P-40, 0.25% sodium deoxycholate, 50 mmol/L NaCl, 50 mmol/L HEPES, 10% glycerol [pH 7.4], 1 mmol/L sodium vanadate, 0.5 mmol/L sodium fluoride, 1 mmol/L phenylmethanesulfonyl fluoride, and protease inhibitor cocktail for general use [Sigma-Aldrich]). Phosphorylation was determined with anti-phospho-tyrosine (p-Tyr) antibody, anti-Src (pY418), and anti-ERK1/2 phospho-specific antibodies. For tyrosine phosphorylation assessment, after immunoblotting for tyrosine phosphorylation, the same membrane was stripped and immunoblotted for actin to serve as loading control. For c-Src phosphorylation assessment, after immunoblotting for phospho-c-Src (p-Src), the same membrane was stripped and immunoblotted for total c-Src (t-Src). Activation of c-Src was expressed as the ratio of p-Src/t-Src with both measurements normalized to 1.0 for the control samples. The assessment of ERK1/2 phosphorylation was performed in the same way as described for c-Src.

### Assessment of Protein Carbonylation

Protein carbonylation was determined by Western blot analysis as we described before.<sup>6</sup> Briefly, an equal amount of total protein from each sample was denatured with 6% SDS (final concentration), derivatized with 2,4-dinitrophenylhydrazine (freshly prepared, 10 mmol/L in 1 N HCl) to form 2,4-dinitrophenyl hydrazone derivatives, and then neutralized with neutralization buffer (30% of glycerol in 2 mol/L Tris). This was followed by Western blot for protein carbonylation assay. The signal density values of control samples were normalized to 1.0 with Ponceau S staining as loading control.

### Western Blotting

For Western blot analysis, equal amounts of total protein were resolved by 10% SDS-PAGE, transferred onto a polyvinylidene difluoride membrane (EMD Millipore), and immunoblotted with indicated antibodies. Signal detection was performed with an enhanced chemiluminescence SuperSignal kit (Pierce, Rockford, IL). Multiple exposures were analyzed to assure that the signals were within the linear range of the film. The signal density was determined using NIH ImageJ 1.48v software.

### Bioinformatics Analysis of the Pro222 of the Na/K-ATPase

DeepView-Swiss-PdbViewer (v4.1) integrated with SWISS-MODEL via the ExpASY web server, a fully automated protein structure homology-modeling server used to generate a 3-dimensional structure of a protein from its amino acid sequence.<sup>24</sup> Modeling of pig Na/K-ATPase E1P and E2P structures was based on 3WGU<sup>25</sup> and 4RES<sup>26</sup> pdb structures, respectively. The pig c-Src kinase crystal structure was

derived from pdb 1Y57.<sup>27</sup> The rat Na/K-ATPase E1P and E2P structures were derived from 3WGU and 4RES. The alignment of pig and rat Na/K-ATPase  $\alpha 1$  subunit showed over 98% sequence similarity. The quality of structures was further assessed by using Structure Analysis and Verification Server (v4). The protein-protein docking analysis was performed by using Z-DOCK web server<sup>28</sup> and the protein-protein interaction was visualized by using Accelrys Discovery Studio Visualizer v2.5.5.

### Statistical Analysis

Data were tested for normality (by SPSS Shapiro-Wilk normality test) and then subjected to parametric analysis. When more than 2 groups were compared, 1-way ANOVA was performed prior to comparison of individual groups, and the post-hoc *t* tests were adjusted for multiple comparisons using Bonferroni's correction. Statistical significance was reported at the  $P < 0.05$  and  $< 0.01$  levels. SPSS software was used for all analysis. Values are given as mean  $\pm$  SEM.

## Results

### Generation of Stable P224A Mutant Cells

As shown in Figure 1, P224A mutant cells expressed a slightly higher but relatively comparable level of mutated rat  $\alpha 1$  in comparison with AAC-19 cells. The expression of rat  $\alpha 1$  was confirmed by a rat  $\alpha 1$ -specific antibody (anti-NASE), and the total  $\alpha 1$  (both endogenous pig  $\alpha 1$  and rat  $\alpha 1$ ) with a generic  $\alpha 1$ -specific antibody  $\alpha 6F$  (Figure 1A). The expression of mutated rat  $\alpha 1$  in P224A mutant cells was predominantly located on the cell surface assayed by immunofluorescence staining of  $\alpha 1$  subunit (data not shown), like AAC-19 and A416P cells.<sup>16</sup> The P224A mutant also expressed a relatively comparable level of  $\beta 1$  subunit in comparison with AAC-19 cells (Figure 1B). The blots were intended to show possible expression difference between AAC-19 and P224A cells, but not to compare the expression of the  $\alpha 1$  subunit to the  $\beta 1$  subunit. [<sup>3</sup>H]-ouabain binding assay was used to assess the cell surface expression level of endogenous pig  $\alpha 1$  subunit in the mutant P224A and A416P cells. The significant lower affinity of ouabain to the rat  $\alpha 1$ , compared to the much higher affinity of ouabain to the pig  $\alpha 1$ , makes it possible to assess the surface expression of pig  $\alpha 1$  in the presence of rat  $\alpha 1$ . In comparison to pig  $\alpha 1$  knockdown PY-17 cells, which express about 8% of endogenous pig  $\alpha 1$  in parent LLC-PK1 cells, AAC-19, P224A, and A416P cells showed significantly lower [<sup>3</sup>H]-ouabain binding level (Figure 1C). A lower [<sup>3</sup>H]-ouabain binding level in P224A mutant cells suggests a further reduction of endogenous pig  $\alpha 1$  subunit compared to PY-17 cells. It is worth noting that PY-17 cells had disrupted Na/K-ATPase/c-Src signaling and did not respond to ouabain

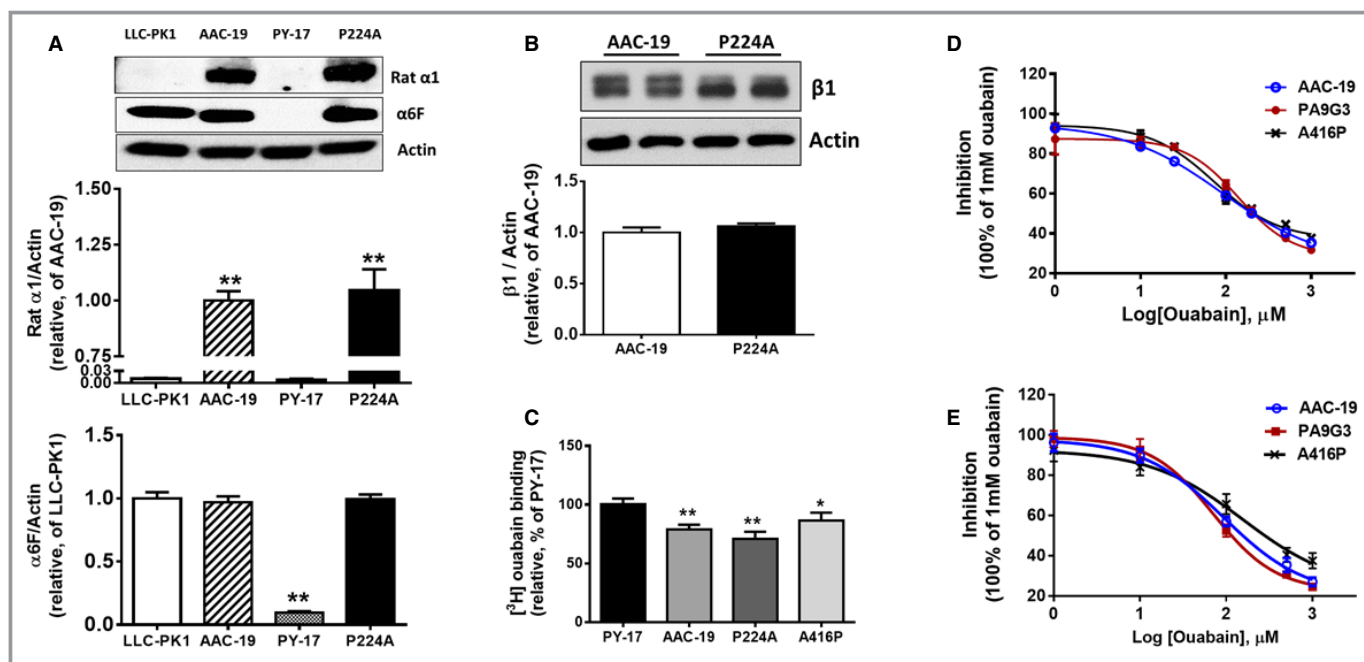


**Figure 1.** Expression of Na/K-ATPase in P224A mutation. A and B, P224A mutant cells express mutated rat  $\alpha 1$  and  $\beta 1$  subunits. Expression of the rat  $\alpha 1$  Na/K-ATPase was determined with polyclonal rat  $\alpha 1$ -specific antibody (anti-NASE) (n=4) and the total  $\alpha 1$  was determined with monoclonal anti- $\alpha 1$  antibody (clone  $\alpha 6F$ ) (n=3). Expression of endogenous pig  $\beta 1$  subunit (glycosylated) was determined with monoclonal anti- $\beta 1$  antibody (clone C464.8) (n=4) and the blots were optimized to show possible difference. A representative Western blot and quantitative analysis were shown. Quantitative analysis (bar graph) showed the relative expression of  $\alpha 1$  and  $\beta 1$  subunits to control wild-type AAC-19 (for rat  $\alpha 1$  and  $\beta 1$ ), and LLC-PK1 (for total  $\alpha 1$ ) cells.  $**P<0.01$  vs control AAC-19 cells. C, [ $^3H$ ]-ouabain binding assay (control value, PY-17 cells,  $922.8\pm 82.1$  CPM/100  $\mu g$  protein), n=4.  $**P<0.01$ ,  $*P<0.05$  vs parent PY-17 cells. (D) Ouabain-sensitive Na/K-ATPase enzymatic activity (control values, in  $\mu mol/L \cdot (mg \text{ protein} \cdot h)^{-1}$ . AAC-19,  $0.953\pm 0.220$ , n=4; P224A,  $2.074\pm 0.169$ , n=3; and A416P  $0.855\pm 0.153$ , n=4), and (E) ouabain-sensitive  $^{86}Rb^+$  uptake assays (control values, in CPM/100  $\mu g$  protein. AAC-19,  $10\ 913.9\pm 1356$ , n=4; P224A,  $14\ 975.7\pm 2149$ , n=4; and A416P  $13\ 426.9\pm 1440$ , n=4). For (C through E), each experiment was performed in triplicate. The values shown were from a typical experiment.

stimulation in terms of c-Src activation,<sup>15,17</sup> suggesting that the remaining endogenous pig  $\alpha 1$  would not interfere with ouabain-mediated signaling and function originated from rat  $\alpha 1$  in AAC-19 and mutant P224A and A416P cells. Functionally, the mutant P224A and A416P cells showed a similar sensitivity to ouabain as AAC-19 cells, in terms of ouabain-sensitive enzymatic activity of the Na/K-ATPase in crude membrane preparations (Figure 1D) as well as the ion-exchange activity assayed by ouabain-sensitive  $^{86}Rb^+$  uptake (Figure 1E). The data indicate that P224A mutation did not change the characteristics of ouabain-induced Na/K-ATPase inhibition.

### Ouabain-Stimulated Protein Tyrosine Phosphorylation

In a different type of cells, ouabain stimulated tyrosine phosphorylation of multiple proteins in a c-Src-dependent manner that is crucial in ouabain-stimulated Na/K-ATPase signaling.<sup>13,29</sup> In contrast to c-Src reconstituted SYF+c-Src cells, depletion of Src family kinases (Src, Yes, and Fyn) prevented ouabain (10–100  $\mu mol/L$ )-induced protein tyrosine

phosphorylation<sup>13</sup> and Na/K-ATPase endocytosis in SYF cells.<sup>19</sup> As shown in Figure 2, ouabain (10  $\mu mol/L$ , 1 hour) significantly stimulated tyrosine phosphorylation of multiple proteins in AAC-19 ( $P<0.01$ ) and A416P ( $P<0.01$ ), but not in P224A cells, suggesting that P224A mutation might prevent ouabain-mediated Na/K-ATPase signaling.

### Ouabain-Stimulated Protein Carbonylation and Na/K-ATPase Signaling

As shown in Figure 3, ouabain (10  $\mu mol/L$ , 1 hour) significantly stimulated ( $P<0.01$ ) protein carbonylation of a broad range of proteins in AAC-19 and A416P but not in P224A cells (Figure 3A). The P224A mutation significantly ( $P<0.01$ ) attenuated ouabain (10  $\mu mol/L$ , 1 hour)-stimulated c-Src and ERK1/2 activation as seen in AAC-19 and A416P mutant cells (Figure 3B and 3C). The ouabain-induced effects in AAC-19 and A416P cells were similar to that seen in LLC-PK1 cells.<sup>6</sup> These data indicate that Pro224 of the rat  $\alpha 1$  subunit might be essential in ouabain-stimulated protein carbonylation and Na/K-ATPase signaling.

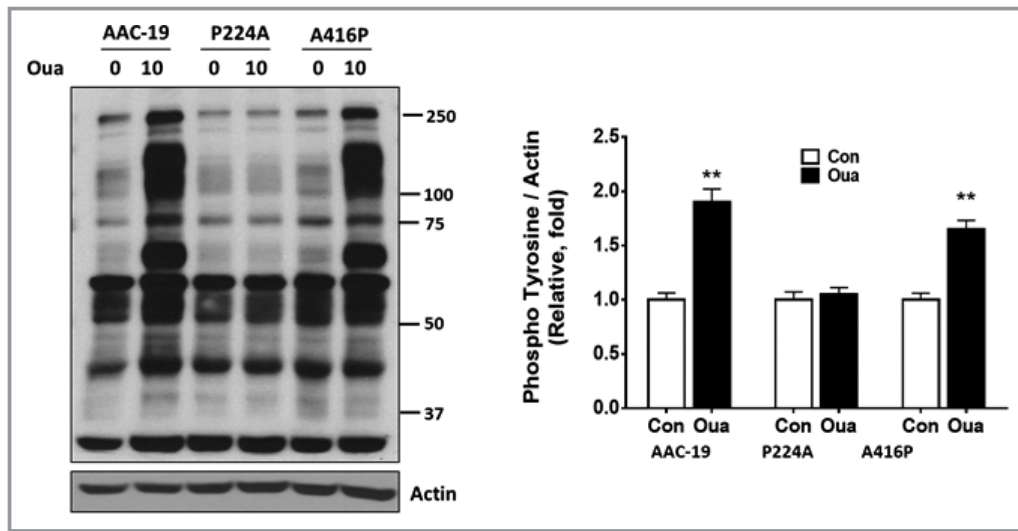


**Figure 2.** P224A mutation prevents ouabain-stimulated protein tyrosine phosphorylation: Ouabain (10 μmol/L, 1 hour)-stimulated protein tyrosine phosphorylation in AAC-19 and A416P mutant cells, but not in P224A mutant cells. A representative Western blot and quantitative analysis were shown. n=4. \*\*P<0.01 vs control.

### Ouabain-Induced Endocytosis of Na/K-ATPase

As shown in Figure 4, in AAC-19 cells, both ouabain (10 μmol/L, 1 hour) and glucose oxidase (GO, 3 mU/mL, 1 hour) stimulated accumulation of Na/K-ATPase α1/β1 subunits in EE fractions (P<0.01), which is consistent with our previous observations in LLC-PK1 cells and rat RPTs.<sup>18,19,23</sup> However, ouabain-induced endocytosis of Na/K-ATPase was significantly attenuated (P<0.01) with the P224A mutation. Functionally, the data are consistent with the observation that ouabain (10 μmol/L, 1 hour)-induced inhibition of active transepithelial <sup>22</sup>Na<sup>+</sup> flux was blunted by the P224A mutation

(Table 2). It is worth noting that both ouabain- and glucose oxidase-stimulated Na/K-ATPase endocytosis was prevented by the P224A mutation, consistent with our previous observation in Src kinase null SYF cells.<sup>6</sup>

### Ouabain-Induced Reduction of Transepithelial <sup>22</sup>Na<sup>+</sup> Transport

In pig LLC-PK1 cells and rat proximal tubular cells, ouabain treatment stimulated internalization of the Na/K-ATPase and NHE3 via the Na/K-ATPase signaling. This led to the reduction

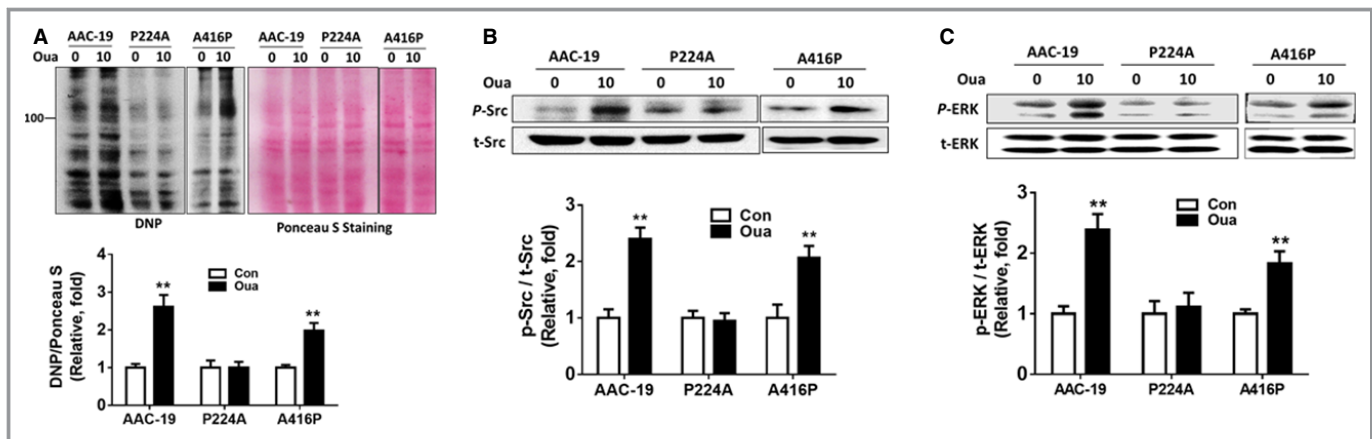


**Figure 3.** P224A mutation prevents ouabain-stimulated protein carbonylation and Na/K-ATPase signaling. Ouabain (Oua, 10 μmol/L, 1 hour)-stimulated protein (A) protein carbonylation (n=5 for AAC-19, n=6 for P224A, and n=4 for A416P cells), (B) activation of c-Src (n=4), and (C) activation of ERK1/2 (n=5 for AAC-19, and n=4 for P224A and A416P cells) in control AAC-19 and mutant A416P cells, but not in P224A cells. Ponceau S staining served as loading control for carbonylation. Activation of c-Src and ERK1/2 was expressed as the ratio of phosphorylated c-Src (p-Src) vs total c-Src (t-Src) and the ratio of phosphorylated ERK1/2 (p-ERK) vs total ERK1/2 (t-ERK), respectively. \*\*P<0.01 vs control. AAC-19 and P224A cells were performed side by side in the same gels, and A416P cells were performed in separated gels. DNP indicates the derivatives of DNPH reaction, i.e. carbonylation.

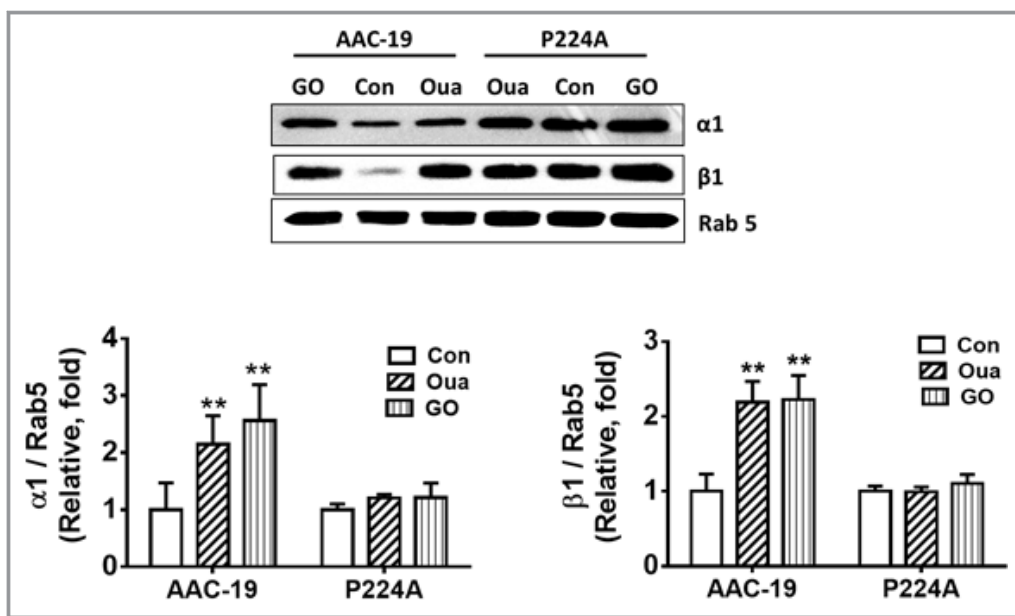


**Figure 4.** P224A mutation prevents ouabain-induced Na/K-ATPase endocytosis. P224A mutation prevents ouabain (10 μmol/L, 1 hour)-stimulated accumulation of α1 and β1 subunit in early endosome fractions. A representative Western blot and quantitative analysis were shown. n=4, \*\*P<0.01 vs control AAC-19 cells.

of the Na/K-ATPase and NHE3 on the cell surface, which further led to reduced Na<sup>+</sup> entry (mainly mediated by NHE3) and Na<sup>+</sup> extrusion (mainly mediated by the Na/K-ATPase) and thus reduced active transepithelial <sup>22</sup>Na<sup>+</sup> transport of the cells.<sup>18,19,23,30–32</sup> To evaluate the effect of the mutation of P224A and A416P on Na/K-ATPase-mediated Na<sup>+</sup> extrusion (by <sup>86</sup>Rb<sup>+</sup> uptake assay), NHE3-mediated Na<sup>+</sup> entry (by H<sup>+</sup>-driven <sup>22</sup>Na<sup>+</sup> uptake assay) and active transepithelial <sup>22</sup>Na<sup>+</sup> transport (by active transepithelial <sup>22</sup>Na<sup>+</sup> flux assay), AAC-19, P224A, and A416P cells were treated with or without ouabain (10 μmol/L, 1 hour) and then the assays were performed. As shown in Table 2, ouabain significantly inhibited the cellular Na<sup>+</sup> entry and extrusion as well as transepithelial <sup>22</sup>Na<sup>+</sup>

transport in AAC-19 and A416P cells, but not in P224A cells. The data indicate that, while ouabain was able to stimulate similar functional changes in AAC-19 and A416P cells, as seen in LLC-PK1 and renal RPTs,<sup>18,23</sup> the P224A mutation prevented ouabain-mediated regulation. However, we could not exclude the possible effect of chloride-coupled cation carriers and K<sup>+</sup> channels.

### Bioinformatics Analysis of the Pro222 of the Na/K-ATPase

The bioinformatics analysis indicated that pig Pro222 carbonylation and Ala222 in Pro/Ala mutation did not affect

**Table 2.** Ouabain (10 μmol/L, 1 Hour)-Inhibited Activities of Na/K-ATPase and NHE3 as Well as Active Transepithelial <sup>22</sup>Na<sup>+</sup> Flux in AAC-19 and A416P Cells, but Not in P224A Mutant Cells

	AAC-19		P224A		A416P	
	Control	Ouabain	Control	Ouabain	Control	Ouabain
<sup>86</sup> Rb <sup>+</sup> uptake	100±6.1	76.4±5.5**	100±3.1	101.9±3.6	100±4.4	80.4±4.2*
H <sup>+</sup> -driven <sup>22</sup> Na <sup>+</sup> uptake	100±4.6	69.7±3.7**	100±5.3	101.0±3.1	100±5.0	71.1±4.5**
Transepithelial <sup>22</sup> Na <sup>+</sup> flux	100±4.7	72.5±5.5**	100±6.7	98.1±3.4	100±5.1	72.3±3.7**

After treatment with or without ouabain (10 μmol/L, 1 hour), assays were performed as described in “Enzymatic and Ion-Exchange Activity Assays” and “Active Transepithelial <sup>22</sup>Na<sup>+</sup> Flux Assay” under “Experimental Methods.” For ouabain-sensitive <sup>86</sup>Rb<sup>+</sup> uptake assay, the control values are (in CPM/100 μg protein) AAC-19, 10 913.9±1356; P224A, 14 975.7±2149; and A416P, 13 426.9±1440. For H<sup>+</sup>-driven <sup>22</sup>Na<sup>+</sup> uptake assay, the control values are (in CPM/100 μg protein) AAC-19, 1721.8±138.7; P224A, 2274.7±109.5; and A416P, 1764.4±150.8. For active transepithelial <sup>22</sup>Na<sup>+</sup> flux assay, 60 minutes after <sup>22</sup>Na<sup>+</sup> was added to the apical compartments, medium from basolateral compartments from each well was collected and counted. The control values are AAC-19, 3236.4±237.7; P224A, 3794.6±219.7; and A416P, 3479.4±250.8. The transepithelial electrical resistance (TER, in Ω·cm<sup>2</sup>) of monolayers was measured in culture medium and calculated by subtracting the resistance measured with the blank insert. The control TER values (in Ω·cm<sup>2</sup>) are AAC-19, 70.8±5.6; P224A, 144.6±8.9; and A416P, 96.9±7.8. Each experiment was performed in triplicate. The control values shown were from a typical experiment. n=3 to 4.

\*P<0.05 and \*\*P<0.01 vs control.

tertiary structure. In comparison to Pro222, carbonylated Pro222 might bind more strongly to c-Src SH2 domain in E1P state. Before carbonylation, both Pro222 and Ala222 were able to bind to Tyr244 of c-Src SH2 domain. After carbonylation, Pro222 was able to bind to Tyr244 as well as other amino acid residues of c-Src SH2 domain, including Asn208, Asn236, and His248. When the  $\alpha 1$  CD2 segment (amino acid residues 152–288) and ND1 segment (amino acid residues 379–435)<sup>13,33</sup> were used for docking analysis, it was predicted that CD2 will bind to the c-Src SH2 domain (amino acid residues 161–251) in both E1P and E2P state, and this appears to be further enhanced by Pro222 carbonylation. However, the ND1 can bind to the c-Src tyrosine kinase domain (amino acid residues 282–531) with many more poses in E1P state than in E2P state. During the E1P to E2P conformation change, the internal distance between the ND1 to pro222 in the  $\alpha 1$  subunit was changed, as indicated by the yellow double-headed arrow (Figure 5, left and right panel), from 24.829 Å in E1P state to 6.340 Å in E2P state. Furthermore, docking analysis with Pro224 and Ala224 in Pro/Ala mutation of rat  $\alpha 1$  showed the same predictions as seen in pig  $\alpha 1$ .

## Discussion

As an ion pump, the physiological function of the Na/K-ATPase is to maintain the electrochemical sodium gradient and cellular sodium homeostasis at the expense of ATP. Recent studies have demonstrated that Na/K-ATPase also functions as a signal transducer through multiple protein–protein interactions.<sup>13,33,34</sup> At physiological concentrations, binding of cardiotonic steroids such as ouabain (at low concentration without significant inhibition of Na/K-ATPase transport activity) to the Na/K-ATPase  $\alpha 1$  subunit results in

the activation of Src, transactivation of epidermal growth factor receptor (EGFR), assembly of multiple protein kinase cascades, and increases in ROS and intracellular calcium (reviewed in<sup>33–36</sup>). The activation of the Na/K-ATPase signaling function is largely independent of the changes in intracellular sodium concentration and significant acute inhibition of Na/K-ATPase transport activity. Functionally, this activation leads to redistribution of Na/K-ATPase and NHE3 in the RPT, resulting in a decrease in surface contents of these 2 transporters and consequently a reduction in RPT sodium reabsorption.<sup>18,19,23,30,31,34,37,38</sup>

Our *in vitro* data suggest that direct carbonylation modification of the Pro222 residue in pig Na/K-ATPase  $\alpha 1$  subunit might be a novel regulatory mechanism of Na/K-ATPase signaling.<sup>6</sup> The Pro residue and  $\alpha 1$  subunit are highly conserved (Table 1). To verify the function of Pro222 carbonylation of pig  $\alpha 1$  subunit in our previous observation,<sup>6</sup> we chose the equivalent Pro224 of rat  $\alpha 1$  subunit to assess its role in ouabain-mediated Na/K-ATPase signaling and subsequent regulation of sodium transport. We constructed the Pro224 to Ala224 (P224A) and Ala416 to Pro416 (A416P) mutants based on a rat  $\alpha 1$  cDNA expressing vector as we described before.<sup>16,17</sup> Using PY-17 cells, which were derived from pig LLC-PK1 cells with an over 90% knockdown of pig  $\alpha 1$  subunit, the ouabain-sensitive endogenous pig  $\alpha 1$  subunit was rescued with ouabain-resistant rat  $\alpha 1$  subunit.<sup>17</sup> The remaining pig  $\alpha 1$  subunit was further reduced by post-transfection selection with ouabain. Wild-type rat  $\alpha 1$ -rescued PY-17 cells (AAC-19)<sup>17</sup> were used as a control. The stable P224A mutant cells (clone 9G3, abbreviated as P224A) and A416P mutant cells (clone 4, abbreviated as A416P) were selected for the following experiments. The establishment and characterization of AAC-19 and A416P cells were described before.<sup>16,17</sup>

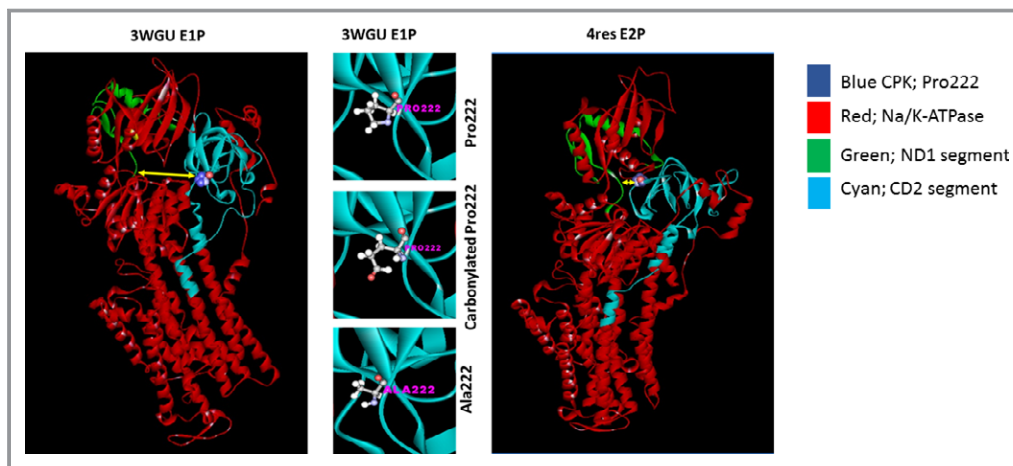


**Figure 5.** Illustration of the 3-dimensional structure of the Na/K-ATPase  $\alpha 1$  subunit in E1P state (left panel), E2P state (right panel), and Pro222 (middle panel). From upper to lower images, Pro222, carbonylated 222, and Ala222 in Pro/Ala mutation in E1P state.



A416 is located in the nucleotide binding (N) domain of the  $\alpha 1$  subunit. Expression of A416P mutant in PY-17 cells showed similar characteristics of AAC-19 cells, such as  $\alpha 1$  and caveolin-1 expressions, ouabain-sensitive Na/K-ATPase activity as well as basal and ouabain-mediated c-Src activation.<sup>16</sup> We reasoned that the A416P mutation can serve as a mutant control.

There are significant differences in sensitivity of the Na/K-ATPase to ouabain based on  $\alpha$  isoforms and species.<sup>39,40</sup> Specifically, the rodent  $\alpha 1$  is far less sensitive than pig, dog, or human  $\alpha 1$ , largely because of the low affinity of ouabain to rodent  $\alpha 1$ . A higher concentration of ouabain (10  $\mu\text{mol/L}$ ) is needed to activate Na/K-ATPase-c-Src cascade and induce Na/K-ATPase endocytosis in primary culture of RPTs isolated from Dahl salt-resistant rats<sup>23</sup> and AAC-19 cells.<sup>32</sup> Since rat  $\alpha 1$  is ouabain resistant, the following experiments were performed with 10  $\mu\text{mol/L}$  ouabain in AAC-19 and mutant cells, which is capable of activating rat Na/K-ATPase signaling without significantly affecting the transport and enzymatic activity of the Na/K-ATPase.<sup>18,32,38</sup>

Our present data demonstrated that altering carbonylation modification of Pro224 of the rat  $\alpha 1$  subunit is able to alter Na/K-ATPase signaling and sodium handling. Rather than contributing to development and maintenance of hypertension, properly regulated RPT Na/K-ATPase signaling has a protective effect under physiological settings.<sup>23,31</sup> The impaired RPT Na/K-ATPase/c-Src signaling in Dahl salt-sensitive rats<sup>23</sup> prompted us to investigate the role of oxidative modification in regulation of Na/K-ATPase signaling and function<sup>6</sup> since an increase in oxidative stress is both a cause and consequence of hypertension<sup>41–45</sup> and contributes to salt sensitivity.<sup>46,47</sup>

In LLC-PK1 cells, ROS is a critical signaling mediator of ouabain-mediated RPT Na/K-ATPase/c-Src signal transduction.<sup>6</sup> Specifically, carbonylation modification of Pro222 of the pig  $\alpha 1$  subunit is involved in the regulation of Na/K-ATPase signal transduction and subsequent inhibition of transepithelial  $^{22}\text{Na}^+$  flux. The present data further indicated that carbonylation modification of the Pro224 of rat  $\alpha 1$  subunit is not only a key regulator but also functions as a signaling amplifier in ouabain-mediated Na/K-ATPase signals and sodium handling. Moreover, ouabain-induced ROS generation and carbonylation modification may function as the link from ouabain-Na/K-ATPase signaling to NHE3 regulation.<sup>6</sup>

An increase in ROS, either induced by ouabain or glucose oxidase, stimulated Src kinase tyrosine phosphorylation<sup>48</sup> and reduced protein content of Na/K-ATPase and NHE3 on the cell surface.<sup>6,8,13</sup> In LLC-PK1 cells, ouabain-mediated inhibition of transepithelial  $^{22}\text{Na}^+$  flux was largely dependent on the coordinated regulation of basolateral Na/K-ATPase and apical NHE3 through Na/K-ATPase signaling.<sup>18,32,49</sup> In LLC-PK1 cells, ouabain reduces cell surface Na/K-ATPase and NHE3

that leads to reduced apical  $\text{Na}^+$  entry through NHE3 and basolateral  $\text{Na}^+$  extrusion through Na/K-ATPase. Disruption of the Na/K-ATPase/c-Src signaling (as seen in pig  $\alpha 1$  knock-down PY-17 cells, caveolin-1 knockout C2-9 cells, and Src kinase null SYF cells) attenuated ouabain-stimulated protein carbonylation.<sup>6</sup> In control AAC-19 and mutant A416P cells, ouabain-induced inhibition of transepithelial  $^{22}\text{Na}^+$  flux was related to the Na/K-ATPase signaling and carbonylation modification. The present study is consistent with our observations in LLC-PK1 cells, suggesting that the Pro224 is a critical mediator of ouabain-stimulated Na/K-ATPase signaling. Functionally, the P224A mutation prevents ouabain-induced Na/K-ATPase signaling, protein carbonylation, and inhibition of transepithelial  $^{22}\text{Na}^+$  flux, further demonstrating the involvement of Pro224 and carbonylation modification in ouabain-mediated effects. The present data strengthen our hypothesis that carbonylation modification of the Pro residue is a novel regulator and an amplifier of Na/K-ATPase signaling and functions. Furthermore, these data support the hypothesis that the Na/K-ATPase/c-Src signaling complex is capable of functioning as a receptor complex of ROS by oxidative modification of the Na/K-ATPase  $\alpha 1$  subunit like carbonylation.

It is well documented that ouabain and other stimuli stimulated c-Src activation. It has been proposed that the Na/K-ATPase  $\alpha 1$  subunit interacts with c-Src kinase to form a functional Na/K-ATPase/c-Src signaling receptor complex.<sup>13,33</sup> In this model, the Na/K-ATPase  $\alpha 1$  subunit provides the ligand binding site and the associated c-Src functions as the kinase moiety. It has also been proposed that c-Src activation is primarily due to an ATP-sparing effect based on a cell-free system.<sup>50,51</sup> While the Na/K-ATPase inhibitors (vanadate and oligomycin) and ATP/ADP ratio regulate c-Src activation, a possible interaction between the  $\alpha 1$  and c-Src was not addressed.<sup>50,51</sup>

There are some additional data that are at odds with our model. It has been shown that ouabain did not induce interaction between the  $\alpha 1$  and c-Src by immunoprecipitation assay in human breast tumor and nontumorigenic cells<sup>52</sup> and ouabain-induced  $\alpha 1$  endocytosis was independent of c-Src activation or PI(3)K in non-small cell lung carcinoma cells.<sup>53</sup> We would point out that these observations are different from those that we have reported in purified pig Na/K-ATPase, primary RPT, SYF and SYF+c-Src, pig LLC-PK1, rat  $\alpha 1$  rescued LLC-PK1, human HK-2, primary culture of human dermal fibroblasts, primary culture of rat cardiac fibroblasts, and a renal fibroblast cell line.\* Therefore, we do believe that the Na/K-ATPase-Src model is worthy of further exploration. Of course, it is possible that the c-Src can be activated by other

\*References 2, 5, 6, 13, 14, 18, 19, 23, 30, 32, 54, 55.

mechanisms and the Na/K-ATPase conformation change is the key step in regulating the endocytosis of this complex, per se.

Our bioinformatic analysis predicted that in pig  $\alpha 1$  subunit, Pro222 carbonylation and Pro222/Ala mutation would not affect the enzymatic function of the Na/K-ATPase, and based on our experimental results, enzymatic function and ouabain sensitivity were unchanged by this mutation. Carbonylation of Pro222 provided more interaction possibilities with c-Src SH2 domain than native Pro222 in E1P state, favoring the interaction between the CD2 domain of  $\alpha 1$  subunit and c-Src SH2 domain. It was also predicted that, while the  $\alpha 1$  CD2 binds to the c-Src SH2 domain in both E1P and E2P state, which was further enhanced by Pro222 carbonylation, the  $\alpha 1$  ND1 binds to c-Src tyrosine kinase domain with more possibilities in E1P state than in E2P state. This suggests that carbonylation might shift a balance between SH2 domain and tyrosine kinase domain binding to the former state, allowing for greater activity of the kinase. However, it is still unclear whether this effect of carbonylation of Pro222 leads to a shift from the E1P→E2P state or whether another mechanism is operant. As prevention of carbonylation at this site by our site mutation prevented activation of c-Src by ouabain, we believe that this carbonylation site may be important in the generation of signals by cardiotonic steroids. We would further speculate that the carbonylation of Pro222 might affect interactions between the  $\alpha 1$  subunit and other signaling partners such as PI3K and the IP3R.<sup>56</sup> However, these predictions need to be further investigated.

Prospectively, carbonylation modification of the Na/K-ATPase, induced by cardiotonic steroids and/or other stimuli, might be important in renal sodium handling. In the kidney, an increase in oxidative stress influenced a number of physiologic processes as aforementioned, including renal sodium handling.<sup>57–61</sup> In RPTs in particular, increases in oxidative stress inhibited the activity of Na/K-ATPase and NHE3 to promote RPT sodium excretion under certain circumstances.<sup>57,59,60</sup> Future studies will be necessary to investigate the role and mechanism of Na/K-ATPase carbonylation in renal sodium handling, especially the reversible carbonylation modification as we have previously observed.<sup>6</sup>

## Sources of Funding

Portions of this work were supported by NIH RO1 HL-109015 (to Z.-j. Xie and J.I. Shapiro), HL071556 (to J.I. Shapiro), and RO1 HL-105649 to (J. Tian and J.I. Shapiro).

## Disclosures

None.

## References

- Xie Z, Kometiani P, Liu J, Li J, Shapiro JI, Askari A. Intracellular reactive oxygen species mediate the linkage of Na<sup>+</sup>/K<sup>+</sup>-ATPase to hypertrophy and its marker genes in cardiac myocytes. *J Biol Chem*. 1999;274:19323–19328.
- Liu J, Tian J, Haas M, Shapiro JI, Askari A, Xie Z. Ouabain interaction with cardiac Na<sup>+</sup>/K<sup>+</sup>-ATPase initiates signal cascades independent of changes in intracellular Na<sup>+</sup> and Ca<sup>2+</sup> concentrations. *J Biol Chem*. 2000;275:27838–27844.
- Tian J, Liu J, Garlid KD, Shapiro JI, Xie Z. Involvement of mitogen-activated protein kinases and reactive oxygen species in the inotropic action of ouabain on cardiac myocytes. A potential role for mitochondrial K(ATP) channels. *Mol Cell Biochem*. 2003;242:181–187.
- Kennedy DJ, Vetteth S, Periyasamy SM, Kanj M, Fedorova L, Khouri S, Kahaleh MB, Xie Z, Malhotra D, Kolodkin NI, Lakatta EG, Fedorova OV, Bagrov AY, Shapiro JI. Central role for the cardiotonic steroid marinobufagenin in the pathogenesis of experimental uremic cardiomyopathy. *Hypertension*. 2006;47:488–495.
- Elkareh J, Kennedy DJ, Yashaswi B, Vetteth S, Shidyak A, Kim EG, Smali S, Periyasamy SM, Harii IM, Fedorova L, Liu J, Wu L, Kahaleh MB, Xie Z, Malhotra D, Fedorova OV, Kashkin VA, Bagrov AY, Shapiro JI. Marinobufagenin stimulates fibroblast collagen production and causes fibrosis in experimental uremic cardiomyopathy. *Hypertension*. 2007;49:215–224.
- Yan Y, Shapiro AP, Haller S, Katragadda V, Liu L, Tian J, Basrur V, Malhotra D, Xie ZJ, Abraham NG, Shapiro JI, Liu J. Involvement of reactive oxygen species in a feed-forward mechanism of Na/K-ATPase-mediated signaling transduction. *J Biol Chem*. 2013;288:34249–34258.
- Liu L, Li J, Liu J, Yuan Z, Pierre SV, Qu W, Zhao X, Xie Z. Involvement of Na<sup>+</sup>/K<sup>+</sup>-ATPase in hydrogen peroxide-induced hypertrophy in cardiac myocytes. *Free Radic Biol Med*. 2006;41:1548–1556.
- Wang Y, Ye Q, Liu C, Xie JX, Yan Y, Lai F, Duan Q, Li X, Tian J, Xie Z. Involvement of Na/K-ATPase in hydrogen peroxide-induced activation of the Src/ERK pathway in LLC-PK1 cells. *Free Radic Biol Med*. 2014;71:415–426.
- Huang WH, Wang Y, Askari A. (Na<sup>+</sup> + K<sup>+</sup>)-ATPase: inactivation and degradation induced by oxygen radicals. *Int J Biochem*. 1992;24:621–626.
- Figtree GA, Liu C-C, Bibert S, Hamilton EJ, Garcia A, White CN, Chia KKM, Cornelius F, Geering K, Rasmussen HH. Reversible oxidative modification: a key mechanism of Na<sup>+</sup>-K<sup>+</sup> pump regulation. *Circ Res*. 2009;105:185–193.
- Petrushanko IY, Yakushev S, Mitkevich VA, Kamanina YV, Ziganshin RH, Meng X, Anashkina AA, Makhro A, Lopina OD, Gassmann M, Makarov AA, Bogdanova A. S-glutathionylation of the Na, K-ATPase catalytic  $\alpha$  subunit is a determinant of the enzyme redox sensitivity. *J Biol Chem*. 2012;287:32195–32205.
- Thévenod F, Friedmann JM. Cadmium-mediated oxidative stress in kidney proximal tubule cells induces degradation of Na<sup>+</sup>/K<sup>+</sup>-ATPase through proteasomal and endo-/lysosomal proteolytic pathways. *FASEB J*. 1999;13:1751–1761.
- Tian J, Cai T, Yuan Z, Wang H, Liu L, Haas M, Maksimova E, Huang XY, Xie ZJ. Binding of Src to Na<sup>+</sup>/K<sup>+</sup>-ATPase forms a functional signaling complex. *Mol Biol Cell*. 2006;17:317–326.
- Liang M, Cai T, Tian J, Qu W, Xie ZJ. Functional characterization of Src-interacting Na/K-ATPase using RNA interference assay. *J Biol Chem*. 2006;281:19709–19719.
- Liang M, Tian J, Liu L, Pierre S, Liu J, Shapiro J, Xie ZJ. Identification of a pool of non-pumping Na/K-ATPase. *J Biol Chem*. 2007;282:10585–10593.
- Lai F, Madan N, Ye Q, Duan Q, Li Z, Wang S, Si S, Xie Z. Identification of a mutant  $\alpha 1$  Na/K-ATPase that pumps but is defective in signal transduction. *J Biol Chem*. 2013;288:13295–13304.
- Taylor NE, Glocka P, Liang M, Cowley AW. NADPH oxidase in the renal medulla causes oxidative stress and contributes to salt-sensitive hypertension in Dahl S rats. *Hypertension*. 2006;47:692–698.
- Cai H, Wu L, Qu W, Malhotra D, Xie Z, Shapiro JI, Liu J. Regulation of apical NHE3 trafficking by ouabain-induced activation of the basolateral Na<sup>+</sup>-K<sup>+</sup>-ATPase receptor complex. *Am J Physiol Cell Physiol*. 2008;294:C555–C563.
- Liu J, Kesiry R, Periyasamy SM, Malhotra D, Xie Z, Shapiro JI. Ouabain induces endocytosis of plasmalemmal Na/K-ATPase in LLC-PK1 cells by a clathrin-dependent mechanism. *Kidney Int*. 2004;66:227–241.
- Soleimani M, Watts BA III, Singh G, Good DW. Effect of long-term hyperosmolality on the Na<sup>+</sup>/H<sup>+</sup> exchanger isoform NHE-3 in LLC-PK1 cells. *Kidney Int*. 1998;53:423–431.
- Orlowski J. Heterologous expression and functional properties of amiloride high affinity (NHE-1) and low affinity (NHE-3) isoforms of the rat Na/H exchanger. *J Biol Chem*. 1993;268:16369–16377.
- Soltoff SP, Mandel LJ. Amiloride directly inhibits the Na, K-ATPase activity of rabbit kidney proximal tubules. *Science*. 1983;220:957–958.

23. Liu J, Yan Y, Liu L, Xie Z, Malhotra D, Joe B, Shapiro JI. Impairment of Na/K-ATPase signaling in renal proximal tubule contributes to Dahl salt-sensitive hypertension. *J Biol Chem*. 2011;286:22806–22813.
24. Biasini M, Bienert S, Waterhouse A, Arnold K, Studer G, Schmidt T, Kiefer F, Cassarino TG, Bertoni M, Bordoli L, Schwede T. SWISS-MODEL: modelling protein tertiary and quaternary structure using evolutionary information. *Nucleic Acids Res*. 2014;42:W252–W258.
25. Kanai R, Ogawa H, Vilsen B, Cornelius F, Toyoshima C. Crystal structure of a Na<sup>+</sup>-bound Na<sup>+</sup>, K<sup>+</sup>-ATPase preceding the E1P state. *Nature*. 2013;502:201–206.
26. Laursen M, Gregersen JL, Yatime L, Nissen P, Fedosova NU. Structures and characterization of digoxin- and bufalin-bound Na<sup>+</sup>, K<sup>+</sup>-ATPase compared with the ouabain-bound complex. *Proc Natl Acad Sci USA*. 2015;112:1755–1760.
27. Cowan-Jacob SW, Fendrich G, Manley PW, Jahnke W, Fabbro D, Liebetanz J, Meyer T. The crystal structure of a c-Src complex in an active conformation suggests possible steps in c-Src activation. *Structure*. 2005;13:861–871.
28. Pierce BG, Wiehe K, Hwang H, Kim BH, Vreven T, Weng Z. ZDOCK server: interactive docking prediction of protein-protein complexes and symmetric multimers. *Bioinformatics*. 2014;30:1771–1773.
29. Haas M, Wang H, Tian J, Xie Z. Src-mediated inter-receptor cross-talk between the Na<sup>+</sup>/K<sup>+</sup>-ATPase and the epidermal growth factor receptor relays the signal from ouabain to mitogen-activated protein kinases. *J Biol Chem*. 2002;277:18694–18702.
30. Liu J, Liang M, Liu L, Malhotra D, Xie Z, Shapiro JI. Ouabain-induced endocytosis of the plasmalemmal Na/K-ATPase in LLC-PK1 cells requires caveolin-1. *Kidney Int*. 2005;67:1844–1854.
31. Periyasamy SM, Liu J, Tanta F, Kabak B, Wakefield B, Malhotra D, Kennedy DJ, Nadoor A, Fedorova OV, Gunning W, Xie Z, Bagrov AY, Shapiro JI. Salt loading induces redistribution of the plasmalemmal Na/K-ATPase in proximal tubule cells. *Kidney Int*. 2005;67:1868–1877.
32. Yan Y, Haller S, Shapiro A, Malhotra N, Tian J, Xie Z, Malhotra D, Shapiro JI, Liu J. Ouabain-stimulated trafficking regulation of the Na/K-ATPase and NHE3 in renal proximal tubule cells. *Mol Cell Biochem*. 2012;367:175–183.
33. Li Z, Xie Z. The Na/K-ATPase/Src complex and cardiotoxic steroid-activated protein kinase cascades. *Pflugers Arch*. 2009;457:635–644.
34. Liu J, Xie ZJ. The sodium pump and cardiotoxic steroids-induced signal transduction protein kinases and calcium-signaling microdomain in regulation of transporter trafficking. *Biochim Biophys Acta*. 2010;1802:1237–1245.
35. Bagrov AY, Shapiro JI, Fedorova OV. Endogenous cardiotoxic steroids: physiology, pharmacology, and novel therapeutic targets. *Pharmacol Rev*. 2009;61:9–38.
36. Schoner W, Scheiner-Bobis G. Endogenous and exogenous cardiac glycosides: their roles in hypertension, salt metabolism, and cell growth. *Am J Physiol Cell Physiol*. 2007;293:C509–C536.
37. Liu J, Periyasamy SM, Gunning W, Fedorova OV, Bagrov AY, Malhotra D, Xie Z, Shapiro JI. Effects of cardiac glycosides on sodium pump expression and function in LLC-PK1 and MDCK cells. *Kidney Int*. 2002;62:2118–2125.
38. Oweis S, Wu L, Kiela PR, Zhao H, Malhotra D, Ghishan FK, Xie Z, Shapiro JI, Liu J. Cardiac glycoside downregulates NHE3 activity and expression in LLC-PK1 cells. *Am J Physiol Renal Physiol*. 2006;290:F997–F1008.
39. Lingrel JB, Kuntzweiler T. Na<sup>+</sup>, K<sup>(+)</sup>-ATPase. *J Biol Chem*. 1994;269:19659–19662.
40. Blanco G, Mercer RW. Isozymes of the Na-K-ATPase: heterogeneity in structure, diversity in function. *Am J Physiol*. 1998;275:F633–F650.
41. Vaziri ND, Rodriguez-Iturbe B. Mechanisms of disease: oxidative stress and inflammation in the pathogenesis of hypertension. *Nat Clin Pract Nephrol*. 2006;2:582–593.
42. Wilcox CS. Oxidative stress and nitric oxide deficiency in the kidney: a critical link to hypertension? *Am J Physiol Regul Integr Comp Physiol*. 2005;289:R913–R935.
43. Touyz RM. Reactive oxygen species, vascular oxidative stress, and redox signaling in hypertension: what is the clinical significance? *Hypertension*. 2004;44:248–252.
44. Welch WJ. Intrarenal oxygen and hypertension. *Clin Exp Pharmacol Physiol*. 2006;33:1002–1005.
45. Kitiyakara C, Chabrashvili T, Chen Y, Blau J, Karber A, Aslam S, Welch WJ, Wilcox CS. Salt intake, oxidative stress, and renal expression of NADPH oxidase and superoxide dismutase. *J Am Soc Nephrol*. 2003;14:2775–2782.
46. Kopkan L, Hess A, Huskova Z, Cervenka L, Navar LG, Majid DS. High-salt intake enhances superoxide activity in eNOS knockout mice leading to the development of salt sensitivity. *Am J Physiol Renal Physiol*. 2010;299:F656–F663.
47. Kopkan L, Majid DS. Superoxide contributes to development of salt sensitivity and hypertension induced by nitric oxide deficiency. *Hypertension*. 2005;46:1026–1031.
48. Giannoni E, Buricchi F, Raugei G, Ramponi G, Chiarugi P. Intracellular reactive oxygen species activate Src tyrosine kinase during cell adhesion and anchorage-dependent cell growth. *Mol Cell Biol*. 2005;25:6391–6403.
49. Liu J, Schuff-Werner P, Steiner M. Double transfection improves small interfering RNA-induced thrombin receptor (PAR-1) gene silencing in DU 145 prostate cancer cells. *FEBS Lett*. 2004;577:175–180.
50. Gable ME, Abdallah SL, Najjar SM, Liu L, Askari A. Digitalis-induced cell signaling by the sodium pump: on the relation of Src to Na<sup>(+)</sup>/K<sup>(+)</sup>-ATPase. *Biochem Biophys Res Commun*. 2014;446:1151–1154.
51. Weigand KM, Swarts HG, Fedosova NU, Russel FG, Koenderink JB. Na, K-ATPase activity modulates Src activation: a role for ATP/ADP ratio. *Biochim Biophys Acta*. 2012;1818:1269–1273.
52. Clifford RJ, Kaplan JH. Human breast tumor cells are more resistant to cardiac glycoside toxicity than non-tumorigenic breast cells. *PLoS One*. 2013;8:e84306.
53. Cherniavsky-Lev M, Golani O, Karlish SJ, Garty H. Ouabain-induced internalization and lysosomal degradation of the Na<sup>+</sup>/K<sup>+</sup>-ATPase. *J Biol Chem*. 2014;289:1049–1059.
54. El-Okdi N, Smaili S, Raju V, Shidyak A, Gupta S, Fedorova L, Elkareh J, Periyasamy S, Shapiro AP, Kahaleh MB, Malhotra D, Xie Z, Chin KV, Shapiro JI. Effects of cardiotoxic steroids on dermal collagen synthesis and wound healing. *J Appl Physiol (1985)*. 2008;105:30–36.
55. Li Z, Cai T, Tian J, Xie JX, Zhao X, Liu L, Shapiro JI, Xie Z. NaKtide, a Na/K-ATPase-derived peptide Src inhibitor, antagonizes ouabain-activated signal transduction in cultured cells. *J Biol Chem*. 2009;284:21066–21076.
56. Yatime L, Laursen M, Morth JP, Esmann M, Nissen P, Fedosova NU. Structural insights into the high affinity binding of cardiotoxic steroids to the Na<sup>+</sup>,K<sup>+</sup>-ATPase. *J Struct Biol*. 2011;174:296–306.
57. Schreck C, O'Connor PM. NAD(P)H oxidase and renal epithelial ion transport. *Am J Physiol Regul Integr Comp Physiol*. 2011;300:R1023–R1029.
58. Han HJ, Lee YJ, Park SH, Lee JH, Taub M. High glucose-induced oxidative stress inhibits Na<sup>+</sup>/glucose cotransporter activity in renal proximal tubule cells. *Am J Physiol Renal Physiol*. 2005;288:F988–F996.
59. Panico C, Luo Z, Damiano S, Artigiano F, Gill P, Welch WJ. Renal proximal tubular reabsorption is reduced in adult spontaneously hypertensive rats: roles of superoxide and Na<sup>+</sup>/H<sup>+</sup> exchanger 3. *Hypertension*. 2009;54:1291–1297.
60. Zhang C, Imam SZ, Ali SF, Mayeux PR. Peroxynitrite and the regulation of Na<sup>+</sup>, K<sup>+</sup>-ATPase activity by angiotensin II in the rat proximal tubule. *Nitric Oxide*. 2002;7:30–35.
61. Juncos R, Hong NJ, Garvin JL. Differential effects of superoxide on luminal and basolateral Na<sup>+</sup>/H<sup>+</sup> exchange in the thick ascending limb. *Am J Physiol Regul Integr Comp Physiol*. 2006;290:R79–R83.